Tensile failure of concrete at high loading rates

Instrumented spalling tests

Dr. Jaap Weerheijm [#*]
Mrs. Ans van Doormaal, Msc [#]
[#]*TNO Prins Maurits Laboratory*
P.O.Box 45, 2280AA Rijswijk, The Netherlands

[*]*Delft University of Technology*
Faculty of Civil Engineering and Geosciences
weerheijm@pml.tno.nl

ABSTRACT: For the numerical prediction of the response of concrete structures under extreme dynamic loading, like debris impact and explosions, reliable material data and material models are essential. TNO-PML and the Delft University of Technology collaborate in the field of impact dynamics and concrete modelling. Recently, TNO-PML developed an alternative SHB test methodology which is based on the old principle of spalling, but up to date equipped with diagnostic tools and to be combined with advanced numerical simulations. Data on dynamic tensile strength and, most important, on fracture energy at loading rates up to 1000 GPa/sec are obtained. The paper describes the test and measurement set-up and presents the new test data. The main focus of the paper is on the reconstruction of the dynamic response and failure process.

Keywords: dynamic loading, rate effects, concrete testing, instrumentation, fracture energy, tensile strength

1 INTRODUCTION

The behavior of concrete under dynamic tensile loading is one of the focal research areas in the joint research programs of TNO-PML and the Delft University of Technology. Hitherto, this resulted a.o. in a model for the rate dependency of the tensile strength and reliable data on the fracture energy. The latter was achieved by a combined experimental and numerical approach. The experiments were performed with the gravity driven Split Hopkinson Bar at the university. The main limitation of this apparatus is the maximum loading rate of about 15 GPa/s (for specimen with a diameter of 75 mm). It was decided to investigate the possibilities to develop an alternative based on the original principle of Hopkinson, i.e. spalling, but up to date equipped with diagnostics and combined with advanced numerical simulations. Data on dynamic tensile strength and on fracture energy at loading rates in the range of 10 –1000 GPa/s are the goal. In the first phase of the research program a method was developed to generate a reproducible loading pulse by means of small explosive charges. The second phase was dedicated to the transmission of the generated loading pulse to the concrete specimen and the recording of the response up to failure. In order to enable independent cross checks in the analysis of the dynamic response, different measurement techniques were applied. Lessons were learned and a third phase was defined in which notched specimen were tested successfully. New test data were obtained on the dynamic tensile strength and, more important, on the dynamic fracture energy.

The paper describes the test set-up and the instrumentation. The main focus is on the results obtained in the third phase of the program and the reconstruction of the dynamic response and failure process in the spall-tests at high loading rates

2 TEST SET-UP

2.1 *Loading device*

Hopkinson presented his ideas of measuring the duration and amplitude of a pressure pulse generated by the impact of a rifle bullet, or a small detonating charge at the end of a cylindrical steel bar (Hopkinson, 1923). He used the spalling phenomenon to capture the loading pulse in an end-segment that was in direct contact with the incident bar but the seam had zero strength. In order to examine the possibilities of this old technique in combination with measurements and numerical simulations, it was decided to apply small detonation charges. The simple test idea is as follows. The charge loads the end of the steel bar and the pressure propagates and impinges a concrete specimen that is situated at the other end of the bar. The transmitted pressure pulse reflects at the free end of the concrete specimen as a tensile pulse and, if the resulting stresses exceed the dynamic strength and the energy criterion is fulfilled, the concrete fails.

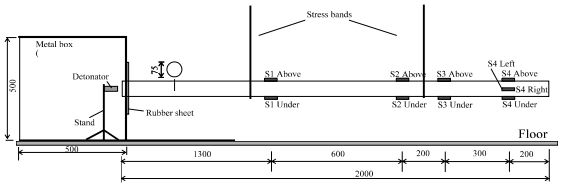

Figure 1. Schematic overview of the test set-up with the locations of the strain gauges. Length and diameter steel bar are 2 m and 75 mm respectively.

In order to determine material properties from this test set-up, the minimum requirements are that the loading pulse is known and can be reproduced. On the other hand the response of the concrete, to this well defined loading pulse, has to be recorded. The test set-up, without the concrete specimen, is given in Figure 1. In order to contain the explosion effects and protect the instrumentation, a steel box (open at one side) was placed around the charge. The strain gauges were shielded with aluminum foil and grounded.

With pressed hexolite charges good results were obtained. A test procedure was established to generate a reproducible loading pulse of sufficient amplitude and strain rate. The characteristics are given in Table 1, while Figure 3a in section 4.1 gives an example of a strain record at location S4, at the end of the steel bar.

Table 1. Characteristics values of loading pulse generated by 10 gram pressed Hexolite at 20 mm stand-off distance.

Maximum strain (μstrain)	Maximum strain rate (1/sec)	Energy (J/m^2)	
		Ascending branch	Up to decreasing strain rate
325 (6.2)#	13.8 (1.46)#	1400	530

Ad #: standard deviation is given in brackets

2.2 *Instrumentation of concrete specimen*

The development of the measurement set-up and background information is given in (Weerheijm et al. 2001 and 2002). The instrumentation consists of:

- Strain gauges on incident steel bar to record the generated loading pulse;
- Strain gauges on the specimen to measure the transmitted compressive loading pulse;
- Carbon pressure gauges and strain gauges in and on the specimen to record the transmitted pulse and the response of the specimen;
- Displacement gauges to record the displacement of the debris as a function of time;
- Video to record the tests.

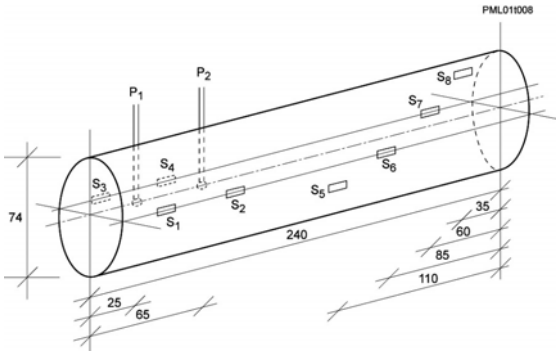

Figure 2 Instrumentation of the concrete specimen

The instrumentation scheme of the un-notched specimen is given in Figure 2. Two carbon gauges are applied near the seam with the steel bar. At these locations the deformation is recorded with 4 strain gauges. Four additional strain gauges are

equally distributed along the rear half of the specimen in order to record the (elastic) response and hopefully to capture the failure zone.

3 TESTS ON INSTRUMENTED CONCRETE SPECIMEN

3.1 *First test series*

In a first series (series B) of twelve tests the instrumentation and the response of concrete have been examined. The results are given in (Weerheijm et al. 2001 and 2002). The main results and conclusions related to the concrete response were:

- The observed strength enhancement at high loading rates (1000 GPa/s) was in accordance with literature;
- The dynamic Young's modulus data showed an unexpected, more pronounced increase than the tendencies reported in literature;
- The transmitted compression pulse does not cause initial damage to the concrete for the applied test conditions;
- The compression pulse appears to be followed by a tension phase. This tension phase was effectively abandoned by the weak plaster seam. Damping in the plaster seam causes damping of the transmitted compression pulse;
- No final failure occurred in the specimen.

3.2 *Second test series (C)*

Based on the observations of the first series, a second test series (C) was defined with the main objective to achieve final failure and to examine the possibilities to collect data of the failure process with the extended measurement set-up. In order to achieve failure the composition of the plaster seam was varied to reduce damping and furthermore, circumferential notches were applied to locate and ensure failure. From the previous tests the most probable location of final failure emerged to be about 70 mm from the end. It was decided to apply a notch depth of 2 and 4 mm at 70 mm from the end. During the test series this decision did not have to be adjusted. The locations of the strain gauges were slightly adjusted to the location of the notch as given in Table 3. The concrete properties are given in Table 4.

Table 2 Tests of series C, applied notch depths and resulting failure

Test number	Notch depth [mm]	Final failure
01spal04	4	yes
01spal05	4	yes
01spal06	4	yes
01spal07	4	yes
01spal08	0	yes
01spal09	0	no
01spal10	2	yes
01spal11	2	yes
01spal12	2	yes
01spal13	0	yes

Table 3 Location centre points of strain gauges 5-8 in test series B and C. Location is given in mm from the free surface.

Strain gauge	Test series B	Test series C
s 5	110	110
s6	85	90
s7	60	50
s8	35	30

Table 4 Static concrete properties of test specimen.

Density, ρ	2350 kg/m^3
Young's modulus, E	37 GPa
Compressive strength, f_c	40 MPa
Tensile strength , f_t	3 MPa
Poison ratio, υ	0.2
Maximum aggregate size	8 mm

4 TEST RESULTS

4.1 *Incident and transmitted pulse, Young's modulus E_{dyn}*

In this section the results of the C-series concerning the damping in the plaster seam and the dynamic Young's modulus are discussed. The transmitted pulse into the specimen is determined from the strain records at the positions 1 - 4 and the wave velocity. The incident loading wave consists of a pressure phase followed by a tensile phase. The tensile phase has to be eliminated else it will lead to immediate tensile failure in the specimen. Therefore, a weak and brittle seam of plaster was applied. Comparison of the records of the incident and transmitted pulse clearly shows the effectiveness of the applied seam. Figure 3 gives the strain records for test 5. For all the tests, the wave velocity was determined using the transmission time between the locations 1/3-2/4, 1/3-5 and 2/4-5. The records at the locations 6-8

were not used because the ascending branch of the records was already affected by the reflected wave at the free end. Comparison of the strain records 1-8 learned that the response in the compression was linear-elastic in most cases. Therefore, the dynamic Young's modulus could be derived from the wave velocity data. The results are given in Table 5.

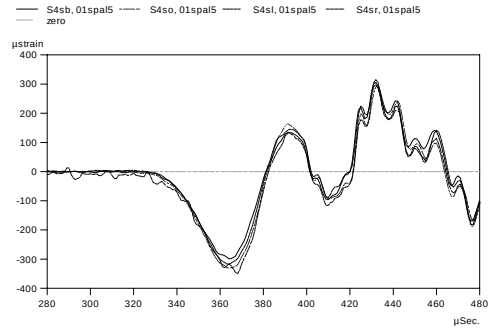

Figure 3.a Strain records incident pulse

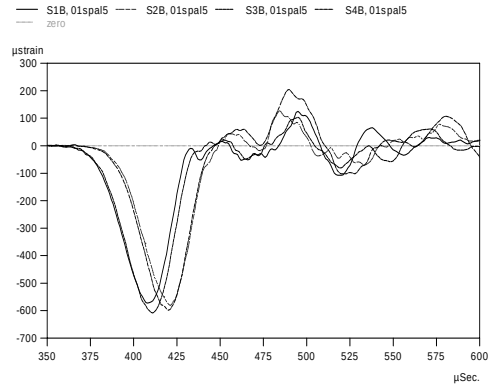

Figure 3.b Strain records transmitted pulse(loc 1-4)

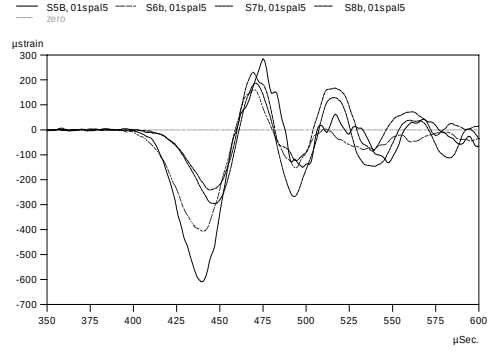

Figure 3.c Strain records transmitted pulse(loc 5-8)

Table 5 Acoustic wave velocity and Young's modulus from strain measurements

C_p	4388 m/s
sdev C_p	255 m/s
E_{dyn}	46.2 GPa

Because the dynamic Young's modulus is known, the amplitude of the transmitted stresses can be calculated from the strain records. But it enables also a cross check. In a linear elastic response without damping the transmitted pulse can be calculated from the incident pulse. The amplitude of the incident pulse is: σ_{inc} = 67 MPa. Without damping, the amplitude of the transmitted pulse is given by the transmission factor α_{tr} that depends on the acoustic impedance values (I = ρ . c) of the steel bar and the concrete specimen.

$$\alpha_{tr} = \frac{2}{1 + I_{steel} / I_{concr}} = 0.413 \qquad (1)$$

σtrans = 0.413 x 67 = 27.7 MPa

The theoretical value equals the value of 27.4, emerging from the strain gauges directly. Apparently no damping occurred in the plaster seam. The conclusion from this result is:

- the damping in the plaster seam can be neglected
- E_{dyn} = 46.2 GPa.

With this firm result for the dynamic Young's modulus, it is interesting to make the comparison with the results published in literature. The strain rate in the C-series is 22.4 1/s. The observed rate effect is (46.2 / 37) = 1.25 while the CEB-formula, see (CEB comite Euro-international du Beton, 1988), predicts a rate effect of 1.4. Both numbers fit into the branch of moderate increase as given in Figure 4 and not the suggested steep increase in this figure.

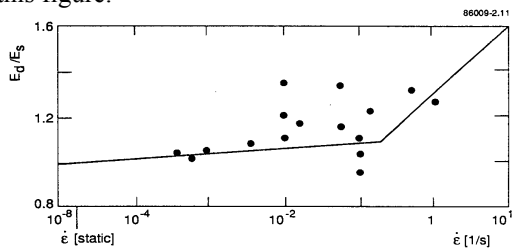

Figure 4 Young's modulus as a function of the strain rate (Dargel, 1984)

4.2 *Reconstruction of the load-deformation relation*

The mechanical material behaviour is characterised and given by the stress-strain relation. In the current test set-up the loading and response recordings are combined or even integrated. In this section the possibilities are described to reconstruct the stress-strain relation from the recordings.

Step 1:
The transferred pressure pulse into the concrete specimen is defined and given by the average of the strain recordings at locations 1-4. It has been observed that no damping occurred in the seam and the transferred pulses, based on linear elastic theory and the recorded pulses were in good agreement with the theoretical value.

The total duration of the pressure pulse is in the order of 70 µsec. The rise time is about 50 µsec and the descending branch takes 20 µsec. With C_p = 4388 m/s the corresponding wave length is in the order of 300 mm. The failure process takes place while the pressure and tensile wave interfere.

To describe and quantify the resulting stress/strain distribution in the specimen it is assumed that the concrete remains linear elastic and does not fail.

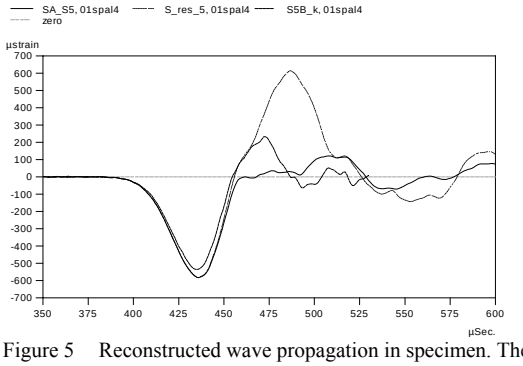

Figure 5 Reconstructed wave propagation in specimen. The incident pressure wave (black), the resulting compression and tension pulse at location 5 (dotted)and the recorded strain at location 5 (dashed).

Step 2:
The pressure pulse propagates through the linear elastic specimen, reflects at the free end as a tensile pulse. Location 5, beyond the tensile failure zone is taken as a reference, and the resulting elastic strain history is determined. Figure 5 gives the result of these interfering waves under the condition that the whole specimen is linear elastic and no failure occurs.

Step 3:
The next step is to combine the theoretical loading pulse at the specific location with the recorded deformation. For location 5 the result is given in Figure 6 with on the vertical axis the stresses using the E_{dyn} value of 46.2 GPa.

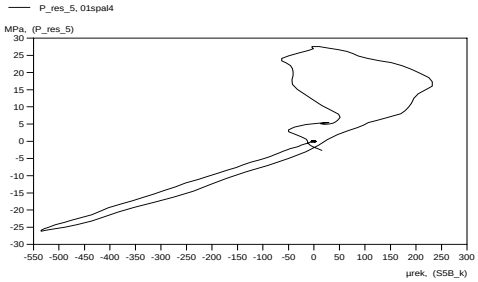

Figure 6 Reconstructed stress-strain curve (test 4-loc 5, beyond the failure zone.

From the reconstructed relations the following conclusions are drawn.

- Damage due to the incident compression pulse is negligible, the material exhibits a linear-elastic behaviour although the amplitude of the residual compression pulse (25 MPa) is about 0.6 f_c and exceeds the static threshold of non-linearity in compression (0.3 f_c). This observation counts for all tests in the C-series. Only a few signals showed some non-linear effects;
- The strain recordings at location 5, beyond the failure zone, can be used to quantify the tensile strength. No evidence was found that non-linear tensile response occurred. Therefore the E_{dyn} and the maximum strain can be used to quantify the dynamic tensile strength;
- Because the deformation of the failure zone itself was recorded, no load-deformation curve could be reconstructed.

4.3 *Reflected tensile pulse, tensile strength $f_{t,dyn}$*

In the previous sections attention was focussed on the transmitted compression pulse in the concrete. Using the strain recordings and the derived value of 46.2 GPa for the Young's modulus, the compression pulse is known and the reflected

tensile pulse can be determined theoretically. Comparison with the strain measurements just outside the failure zone gives information on the dynamic tensile strength.

The reflected pulses caused failure in all tests except test 9. For the un-notched specimen failure occurred in the zone of the measuring locations 6 and 7. Also for the notched tests permanent deformation was recorded at these locations. Most reliable information about the tensile strength follows from strain record number 5 when no residual deformation is recorded. For the notched specimen the area reduction has been taken into account. The dynamic load conditions and observed tensile strengths are given in Table 6. The overall observed rate effect is:

f_{dyn}/f_{stat} = 5.3

at the rate of : 22.5 1/s or 1050 GPa/s

Table 6 Strain amplitudes at location 5 and the dynamic strength for the tests without residual deformation

Notch depth mm	Num-ber of tests	Sb-5 μstrain	$f_{tension}$ MPa	strain rate 1/s	load rate GPa/s
0	3				
Average		399	18.4	20.0	920
Stdev		31	1.4	2.6	103
2	3				
Average		343	17.7	21.3	988
Stdev		63	3.2	3.2	152
4	4				
Average		251	14.5	25.5	1166
Stdev		26	1.5	6.5	299
All tests	10				
Average		315	15.8	22.5	1039
Sdev		73	3.2	3.8	177

It should be noted that due to the application of the geometrical discontinuity at the notch, stress concentrations are introduced leading to early crack initiation and reduced specimen strength. The effect of the notches on the dynamic strength can not be quantified at this stage. It is possible that at the high loading rates the inertia effects at small scale, leading to the steep strength increase, dominate the failure process and stress concentrations have a minor effect on the observed specimen strength. Detailed numerical modeling is needed to quantify the effect. Comparison of the few data that were gathered in the current series indicates that the dynamic strength of the 4-mm notched specimens was affected by the notches and is not representative for the material strength. It is concluded that the rate effect of 5.3 on the tensile strength is a lower bound value for the true dynamic material response. Figure 7 gives the rate dependency from literature and previous research and shows the consistency with the current data.

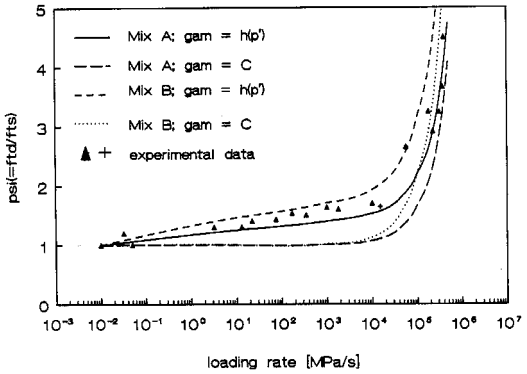

Figure 7 Rate effect on uniaxial tensile strength

4.4 *Fracture energy, $G_{f,dyn}$*

Beside the dynamic tensile strength, the aim of the current test-set up is to gather data on the dynamic fracture energy. Failure occurs when the strength criterion is fulfilled and sufficient energy is available, and can be released into the fracture zone to establish complete failure. From previous research it is known that the fracture energy of the applied concrete for static loading is in the order of 100 J/m^2. In the B-series no final failure occurred because the energy transferred to the failure zone was too small to fulfil the energy criterion. In the C-series final failure occurred. From these tests, however, no direct information about the fracture energy is available because the deformation of the failure zone was not measured like in the previous research with the gravity driven SHB (Weerheijm, 1992). The measurement data have been analysed in several ways in order to learn about the dynamic failure process and see what quantitative information can be derived from the strain and velocity measurements. These analyses have been reported in (Weerheijm et al. 2003). Because the quantitative results for the analyses were about the same, in this paper only one method is given.

First step in the analysis is to make the following assumptions:

- only one fracture zone occurs, which is located at the notch;
- the concrete specimen is undamaged, and is linear–elastic except in the fracture zone. Consequently, all energy absorption takes place in the fracture zone;
- the width of the fracture zone, l_{frac}, is in the order of 20 mm (Weerheijm et al. 2003).

During the failure process, deformation and kinetic energy of the surrounding material is released into the fracture zone and cracks are formed. The failure zone is defined as the zone in which the material is involved in the energy exchange process. It should be noted that the width of the failure zone, l_{fail}, is larger than l_{frac}.

One of the options to estimate the dynamic fracture energy from the tests is given by the gross energy balance of the specimen. The energy balance can be made based on the compression pulse, the energy trapped in the spall debris, the tensile pulse beyond the failure zone and the unknown fracture energy. In symbols:

$$E_{compr} = E_{,debr} + E_{trans\ tens} + E_{fract}$$

The assumption is that all the material is linear elastic except the failure zone. All energy dissipation is concentrated in the failure zone and contributes to E_{fract} (= G_f). The energy terms, E_{vv} +E_{kin}, for the stress pulses are determined using the dynamic Young's modulus value of 46.2 GPa and the positive phase of the recorded pulses at the locations 1-4 and 5 for the compression and tension pulse respectively.

$$E_{vv} = \frac{1}{2} \cdot E \cdot \int \varepsilon^2(x) dl_{pulse}$$

$$E_{kin} = \frac{1}{2} \cdot \int \rho \cdot v^2(x) \cdot dl_{pulse}$$

and because $v = \sqrt{\left(E/\rho\right)} \cdot \varepsilon$

$E_{kin} = E_{vv}$ for LE materials.

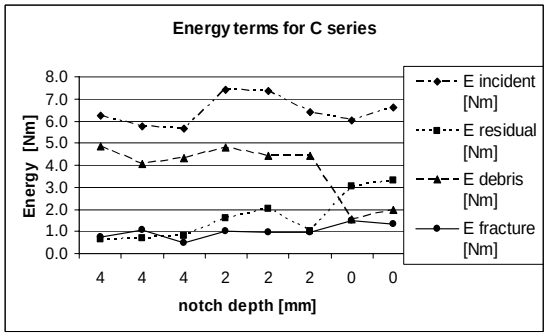

Figure 8 Energy terms of gross energy balance for the various notch depths

The kinetic energy of the spall debris follows from displacement measurements and the spall mass. The displacement measurement signals initially show a strong fluctuation, the velocity is derived after about 10 msec. The initial velocity is underestimated by this procedure. The assumption is that the displacement measurements are still representative for the first moments after final failure when stress waves still run through the spall debris. Because the spall debris is linear elastic, E_{debr} is given by twice the calculated kinetic energy. Figure 8 gives the results for the energy terms while the derived G_f values for the gross and nett section are given in Figure 9.

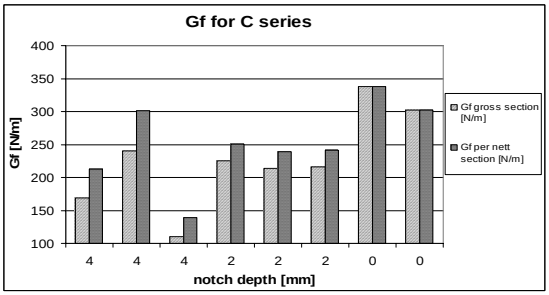

Figure 9 Fracture energy related to the gross and nett cross section.

The results show that :

- G_f for the notched specimen < 250 J/m^2 , except one test;
- The results obtained from the gross energy balance are quite sensitive to the displacement, velocity measurements of the spall debris. In the current set-up the velocity and the kinetic energy are underestimated, resulting in an overestimation of the fracture energy

- The results show that the 2-mm notch tests give consistent results for the fracture energy;
- Using the 2 mm –notch results and the assumption that all the dissipated energy contributes to the fracture energy of the single failure zone, a new upper bound for the fracture energy is obtained:
- $G_{f,\ dyn} < 250\ J/m^2$ at loading rates of 1000 GPa/s

5 CONCLUDING REMARKS

The main results of these phases are:

- An experimental set-up has been accomplished to quantify dynamic tensile properties of concrete at high loading rates. New information and data are obtained for the regime of loading rates of 1000 GPa/s for which hardly any data was available;
- The old Hopkinson bar technique combined with sophisticated instrumentation offers good perspective to study the dynamic failure process in tension;
- For the selected test conditions loading rates in concrete are in the order of 1000 GPa/s. The observed enhancement factors for the tensile strength and the Young's modulus (compression) were 5.3 and 1.2 respectively. The results are in accordance with trends reported in literature.
- The measurement set-up enabled the quantification of all terms of the gross energy balance of the test set-up and an upper limit for the dynamic fracture energy was derived. The maximum enhancement factor for the fracture energy is 2.5 at loading rates of 1000 GPa/s. Previous research learned that for loading rates up to 15 GPa/s the fracture energy does not increase.

6 REFERENCES

Weerheijm,J. & Doormaal, J.C.A.M. van, Development of new test set-up for dynamic tensile tests on concrete at high loading rates, 10th International Symposium on Interaction of the Effects of Munitions with Structures, 2001

Weerheijm, J. et al. Development of a new test set-up for dynamic tensile tests on concrete under high loading rates Part 1: Results test series A. TNO-PML report, 2002.

Hopkinson, B. Collective scientific papers. Cambridge University Press, 1921

Kolski, H. Stress Waves in Solids, Clarendon Press, Oxford, pp221, 1953

Johnson, W. Impact strength of Materials, Edward Arnold (Publishers) Limited, 1972

Landon, J.W. and Quinney, H. Experiments with the Hopkinson Pressure Bar. Proc. Research Society, A 103, 622, 1923

Weerheijm, J. Concrete under impact tensile loading and lateral compression. Doctoral thesis, Delft University, 1992.

Ross, C.A. The effects of Dynamic Pre-compression on the dynamic Tensile Strength of Concrete and Mortar. ASME Conference publication PVP-Vol 361, pp. 31-36, 1998

CEB comite Euro-international du Beton, Concrete structures under impact and impulsive loading (synthesis report), Bulletind'information no. 187; August 1988

Dargel, H.J. Zur rechnerischen Analyse von Stahl-betontragwerken unter stossartiger Beanspruchung. Doctoral thesis, Darmstadt University, 1984

Doormaal, J.C.A.M. van. and Weerheijm, J. Ultimate deformation capacity of reinforced concrete slabs under blast load. Presented at: Structures Under Shock and Impact IV (SUSI IV), Udine, IT, 3-5 July 1996.

Weerheijm, J. et al. Development of a new test set-up for dynamic tensile tests on concrete under high loading rates Part 1: Results and evaluation of test series B and C. TNO-PML report, 2003.